

Displaced Maxwellian Calculation of Transport in *n*-Type GaAs†

W. HEINLE

AEG-Telefunken Forschungsinstitut, 79 Ulm, Federal Republic of Germany

(Received 4 October 1968)

In the approximation of displaced Maxwell electron distribution functions, the relative importance of the various lattice scattering processes to energy and momentum relaxation is investigated theoretically for *n*-type GaAs as a function of electric field, taking into account the nonparabolic structure of the (0,0,0) valley. In this valley, at room temperature, energy and momentum relaxation is found to be governed by polar optical scattering below ~ 7 kV/cm and by nonequivalent intervalley scattering between the (0,0,0) and (1,0,0) valleys above (for a deformation potential of 5×10^8 eV/cm). In the (1,0,0) valleys, polar intravalley and equivalent and nonequivalent intervalley scattering are significant for the energy relaxation in like manner, whereas equivalent intervalley scattering is predominant for the momentum relaxation (for an equivalent intervalley scattering constant of 10^9 eV/cm). The conservation equations for energy, momentum, and particle number are used to calculate the field-dependent relative population of the (1,0,0) valleys, the mobilities, the electron temperatures, the diffusion coefficients, and the field dependence of the average drift velocity; the effect of nonparabolicity on these results is discussed. Evidence is found against a nonequivalent intervalley-scattering deformation potential as low as 1×10^8 eV/cm.

I. INTRODUCTION

THE transport properties of *n*-type GaAs, especially the mobilities as a function of field, have found great interest lately because of the Gunn effect. A recent calculation,¹ which was based upon the assumption of quasi-elasticity of the polar optical intravalley and the acoustical intervalley scattering between the (0,0,0) (central) and (1,0,0) (satellite) valleys, determined the electron distribution functions from a system of coupled differential equations derived from the Boltzmann equation. These computations provided, in particular, the shape of the drift-velocity-versus-field characteristic, which is typical of the Gunn effect, with a region of negative slope, but with threshold and peak-drift-velocity values (depending on the coupling constants for the various scattering mechanisms) that are too low in comparison with most of the experiments (for a representation of experimental curves see, e.g., Ref. 1). Treating the (1,0,0) valley electrons as thermal, rather than hot,¹ slightly increases these quantities²; however, there still remains a discrepancy concerning the drift-velocity scale. Better agreement is obtained by a calculation using displaced Maxwellians,³ although there is an indication that the assumption of such distribution functions is not quite correct for the electron concentrations usually encountered in the Gunn effect.^{4,5} Because of the relative simplicity of the calculation and the good quality of the results, the mobilities, electron temperatures, and population ratio have been calculated as a function of field on this basis; thereby, in contrast to Ref. 3, the nonparabolicity of the (0,0,0) valley also has been considered, and the contribution of the differ-

ent lattice scattering mechanisms to energy and momentum relaxation is analyzed.

II. CALCULATION

The nonparabolicity of the (0,0,0) valley in GaAs is described by^{6,7}

$$\hbar^2 k_c^2 = 2m_0\epsilon(a_1 + a_2\epsilon) \quad (1)$$

for electron energies ϵ up to a few eV, where

$$m_0 = \text{free-electron mass,} \\ a_2 \simeq 0.040 \text{ eV}^{-1},$$

and the subscripts *c* and *s* refer to *central* and *satellite* valley, respectively. The satellite valleys are assumed to be spherical and parabolic. The relevant scattering mechanisms to be considered are polar optical and acoustical intravalley scattering for both kinds of valleys, equivalent intervalley scattering between the (1,0,0) minima (*ss'*), and nonequivalent scattering between the (0,0,0) valley and the (1,0,0) valley (*cs*). The collision operators for spherical but arbitrarily nonparabolic band structure have been derived several times.^{1,8,9} Hence, the average values for the energy and momentum transfer to the lattice, $\langle d\epsilon/dt \rangle_{\text{coll}}$ and $\langle dp/dt \rangle_{\text{coll}}$, can be derived for the two-term expansion of a displaced Maxwell distribution

$$f(\epsilon, \cos\vartheta) \equiv A \exp\left(-\frac{\epsilon(|\mathbf{k}-\mathbf{k}_d|)}{k_0 T}\right) \\ \simeq A \left(1 + \frac{2kk_d \cos\vartheta}{k_0 T} \frac{d\epsilon}{dk^2}\right) \exp\left(-\frac{\epsilon(k)}{k_0 T}\right),$$

† Work supported by the Federal Ministry of Defense as a part of Research Contract No. T-710-I-203.

¹ E. M. Conwell and M. O. Vassell, *Phys. Rev.* **166**, 797 (1968).

² W. Heinle, *Z. Physik* (to be published).

³ P. N. Butcher and W. Fawcett, *Phys. Letters* **21**, 489 (1966).

⁴ E. M. Conwell and M. O. Vassell, *IEEE Trans. Electr. Dev.* **ED-13**, 22 (1966).

⁵ A. D. Boardman, W. Fawcett, and H. D. Rees, *Solid State Commun.* **6**, 305 (1968).

⁶ H. Ehrenreich, *Phys. Rev.* **120**, 1951 (1960).

⁷ E. M. Conwell and M. O. Vassell, *Phys. Letters* **25A**, 302 (1967).

⁸ I. M. Dykman and P. M. Tomchuk, *Fiz. Tverd. Tela* **8**, 1343 (1966) [English transl.: *Soviet Phys.—Solid State* **8**, 1075 (1966)].

⁹ D. Matz, *J. Phys. Chem. Solids* **28**, 373 (1967).

where

ϑ = angle between wave vector \mathbf{k} and electric field \mathbf{E} ,
 A = normalization constant,
 k_0 = Boltzmann constant,

T = electron temperature,
 $\hbar\mathbf{k}_d$ = drift crystal momentum,

in a direct but tedious way, so that it may be sufficient to present only the final results:

$$\begin{aligned} \left\langle \frac{d\epsilon}{dt} \right\rangle_{ac,c} &\equiv -\frac{E_1^2 \hbar (1 - T_0/T_c) A_c}{\rho q_c} \int_0^\infty [k_c^2(\epsilon) k_c^{2'}(\epsilon)]^2 \exp\left(-\frac{\epsilon}{k_0 T_c}\right) d\epsilon, \\ \left\langle \frac{d\epsilon}{dt} \right\rangle_{pol,c} &\equiv -\frac{\pi e^2 \hbar \omega_0^2 N_0 A_c}{\tilde{\epsilon} q_c} \left\{ \exp\left[\frac{\hbar \omega_0}{k_0} \left(\frac{1}{T_0} - \frac{1}{T_c}\right)\right] - 1 \right\} \\ &\quad \times \int_0^\infty k_c^{2'}(\epsilon) k_c^{2'}(\epsilon + \hbar \omega_0) \exp\left(-\frac{\epsilon}{k_0 T_c}\right) \ln \frac{k_c(\epsilon + \hbar \omega_0) + k_c(\epsilon)}{k_c(\epsilon + \hbar \omega_0) - k_c(\epsilon)} d\epsilon, \\ \left\langle \frac{d\epsilon}{dt} \right\rangle_{field,c} &\equiv -e E v_{dc}, \\ \left\langle \frac{dp}{dt} \right\rangle_{ac,c} &\equiv \frac{2E_1^2 T_0 k_{dc} A_c}{3\rho s^2 T_c q_c} \int_0^\infty k_c^4(\epsilon) k_c^{2'}(\epsilon) \exp\left(-\frac{\epsilon}{k_0 T_c}\right) d\epsilon, \\ \left\langle \frac{dp}{dt} \right\rangle_{pol,c} &\equiv -\frac{\pi \hbar \omega_0 e^2 N_0 k_{dc} A_c}{3\tilde{\epsilon} k_0 T_c q_c} \int_0^\infty \left\{ \ln \frac{k_c(\epsilon + \hbar \omega_0) + k_c(\epsilon)}{k_c(\epsilon + \hbar \omega_0) - k_c(\epsilon)} \cdot [k_c^2(\epsilon) - k_c^2(\epsilon + \hbar \omega_0)] \right. \\ &\quad \times \left. \left\{ k_c^{2'}(\epsilon) \exp\left[\frac{\hbar \omega_0}{k_0} \left(\frac{1}{T_0} - \frac{1}{T_c}\right)\right] - k_c^{2'}(\epsilon + \hbar \omega_0) \right\} \right. \\ &\quad \left. \left. - 2k_c(\epsilon) k_c(\epsilon + \hbar \omega_0) \left\{ k_c^{2'}(\epsilon) \exp\left[\frac{\hbar \omega_0}{k_0} \left(\frac{1}{T_0} - \frac{1}{T_c}\right)\right] + k_c^{2'}(\epsilon + \hbar \omega_0) \right\} \right\} \exp\left(-\frac{\epsilon}{k_0 T_c}\right) d\epsilon, \\ \left\langle \frac{dp}{dt} \right\rangle_{field,c} &\equiv -e E. \end{aligned} \tag{2}$$

Here,

$-e$ = electron charge,
 ρ = mass density,
 s = sound velocity,

E_1 = deformation potential constant for acoustical phonon scattering,

ω_0 = angular frequency of the polar optical phonon,

$N_0 = 1/[\exp(\hbar \omega_0/k_0 T_0) - 1]$,

$1/\tilde{\epsilon} = 1/\epsilon_\infty - 1/\epsilon_0$; ϵ_0 , ϵ_∞ being the zero- and high-frequency dielectric constants, respectively,

v_d = drift velocity,

T_0 = lattice temperature.

The prime denotes differentiation with respect to the argument. q_c is the normalization integral for the central valley, representing its relative population if the normalization is chosen according to Eq. (6). k_c is given by Eq. (1); on specializing to $k_c \rightarrow k_s$ (i.e., $a_2 \rightarrow 0$, $a_1 \rightarrow m_s/m_0$), the above formulas go over to the familiar expressions for parabolic band structure as being valid for the satellite minima. In addition, one has for intervalley scattering

$$\begin{aligned} \left\langle \frac{d\epsilon}{dt} \right\rangle_{c \leftrightarrow s,c} &\equiv \frac{(\Xi_{cs}/a_0)^2 \nu_s A_c}{2\rho \omega_{cs} q_c} \int_0^\infty \left[(N_{cs} + 1)(\epsilon + \Delta - \hbar \omega_{cs}) k_c(\epsilon + \Delta - \hbar \omega_{cs}) k_c^{2'}(\epsilon + \Delta - \hbar \omega_{cs}) \right. \\ &\quad \times \left. \left\{ \frac{A_s}{A_c} \exp\left(-\frac{\epsilon}{k_0 T_s}\right) - \exp\left[-\frac{\epsilon + \Delta}{k_0 T_c} + \frac{\hbar \omega_{cs}}{k_0} \left(\frac{1}{T_c} - \frac{1}{T_0}\right)\right] \right\} \right. \\ &\quad \left. + N_{cs}(\epsilon + \Delta + \hbar \omega_{cs}) k_c(\epsilon + \Delta + \hbar \omega_{cs}) k_c^{2'}(\epsilon + \Delta + \hbar \omega_{cs}) \right. \\ &\quad \left. \times \left\{ \frac{A_s}{A_c} \exp\left(-\frac{\epsilon}{k_0 T_s}\right) - \exp\left[-\frac{\epsilon + \Delta}{k_0 T_c} - \frac{\hbar \omega_{cs}}{k_0} \left(\frac{1}{T_c} - \frac{1}{T_0}\right)\right] \right\} \right] k_s(\epsilon) k_s^{2'}(\epsilon) d\epsilon, \end{aligned}$$

$$\left\langle \frac{d\epsilon}{dt} \right\rangle_{s \leftrightarrow c, s} \equiv \frac{(\Xi_{cs}/a_0)^2 A_s}{2\rho\omega_{cs}} \frac{A_c}{q_s} \int_0^\infty \left\{ \frac{A_c}{A_s} \exp\left(-\frac{\Delta+\epsilon}{k_0 T_c}\right) \left[(N_{cs}+1) \exp\left(-\frac{\hbar\omega_{cs}}{k_0 T_c}\right) k_c(\epsilon+\Delta+\hbar\omega_{cs}) k_c^{2'}(\epsilon+\Delta+\hbar\omega_{cs}) \right. \right. \\ \left. \left. + N_{cs} \exp\left(\frac{\hbar\omega_{cs}}{k_0 T_c}\right) k_c(\epsilon+\Delta-\hbar\omega_{cs}) k_c^{2'}(\epsilon+\Delta-\hbar\omega_{cs}) \right] - [N_{cs} k_c(\epsilon+\Delta+\hbar\omega_{cs}) k_c^{2'}(\epsilon+\Delta+\hbar\omega_{cs}) \right. \right. \\ \left. \left. + (N_{cs}+1) k_c(\epsilon+\Delta-\hbar\omega_{cs}) k_c^{2'}(\epsilon+\Delta-\hbar\omega_{cs}) \right] \exp\left(-\frac{\epsilon}{k_0 T_s}\right) \right\} \epsilon k_s(\epsilon) k_s^{2'}(\epsilon) d\epsilon, \quad (3)$$

$$\left\langle \frac{dp}{dt} \right\rangle_{c \rightarrow s, c} \equiv \frac{(\Xi_{cs}/a_0)^2 \nu_s \hbar k_{dc} A_c}{3\rho\omega_{cs} k_0 T_c} \frac{A_c}{q_c} \exp\left(-\frac{\Delta}{k_0 T_c}\right) \int_0^\infty \left[N_{cs} \exp\left(\frac{\hbar\omega_{cs}}{k_0 T_c}\right) k_c^3(\epsilon+\Delta-\hbar\omega_{cs}) \right. \\ \left. + (N_{cs}+1) \exp\left(-\frac{\hbar\omega_{cs}}{k_0 T_c}\right) k_c^3(\epsilon+\Delta+\hbar\omega_{cs}) \right] k_s(\epsilon) k_s^{2'}(\epsilon) \exp\left(-\frac{\epsilon}{k_0 T_c}\right) d\epsilon,$$

$$\left\langle \frac{dp}{dt} \right\rangle_{s \rightarrow c, s} \equiv \frac{(\Xi_{cs}/a_0)^2 \hbar k_{ds} A_s}{3\rho\omega_{cs} k_0 T_s} \frac{A_s}{q_s} \int_0^\infty \left[N_{cs} k_c(\epsilon+\Delta+\hbar\omega_{cs}) k_c^{2'}(\epsilon+\Delta+\hbar\omega_{cs}) \right. \\ \left. + (N_{cs}+1) k_c(\epsilon+\Delta-\hbar\omega_{cs}) k_c^{2'}(\epsilon+\Delta-\hbar\omega_{cs}) \right] k_s^3(\epsilon) \exp\left(-\frac{\epsilon}{k_0 T_s}\right) d\epsilon,$$

and for the sake of completeness,

$$\left\langle \frac{d\epsilon}{dt} \right\rangle_{s \rightarrow s', s} \equiv -\frac{2(\Xi_{ss'}/a_0)^2 (\nu_s - 1) m_s^3 k_0 T_s \omega_{ss'} N_{ss'} A_s}{\rho \hbar^4} \frac{A_s}{q_s} \exp\left(\frac{\hbar\omega_{ss'}}{2k_0 T_s}\right) \left\{ \exp\left[\frac{\hbar\omega_{ss'}}{2k_0} \left(\frac{1}{T_0} - \frac{1}{T_s}\right)\right] - 1 \right\} K_1\left(\frac{\hbar\omega_{ss'}}{2k_0 T_s}\right), \\ \left\langle \frac{dp}{dt} \right\rangle_{s \rightarrow s', s} \equiv \frac{2(\Xi_{ss'}/a_0)^2 (\nu_s - 1) m_s^3 \omega_{ss'} N_{ss'} k_{ds} A_s}{3\rho \hbar^3} \frac{A_s}{q_s} \exp\left(\frac{\hbar\omega_{ss'}}{2k_0 T_s}\right) \left[\left\{ 1 + \exp\left[\frac{\hbar\omega_{ss'}}{k_0} \left(\frac{1}{T_0} - \frac{1}{T_s}\right)\right] \right\} K_0\left(\frac{\hbar\omega_{ss'}}{2k_0 T_s}\right) \right. \\ \left. + \left\{ \exp\left[\frac{\hbar\omega_{ss'}}{k_0} \left(\frac{1}{T_0} - \frac{1}{T_s}\right)\right] \left(\frac{4k_0 T_s}{\hbar\omega_{ss'}} + 1\right) + \left(\frac{4k_0 T_s}{\hbar\omega_{ss'}} - 1\right) \right\} K_1\left(\frac{\hbar\omega_{ss'}}{2k_0 T_s}\right) \right],$$

where

- ω_{cs} = angular frequency of the nonequivalent intervalley phonon,
- $N_{cs} = 1/[\exp(\hbar\omega_{cs}/k_0 T_0) - 1]$,
- Δ = energy separation of the bottoms of the (1,0,0) and (0,0,0) valleys,
- Ξ_{cs} = nonequivalent intervalley-scattering deformation potential,
- a_0 = lattice constant,
- $\omega_{ss'}$ = angular frequency of the equivalent intervalley phonon,
- $N_{ss'} = 1/[\exp(\hbar\omega_{ss'}/k_0 T_0) - 1]$,
- $\Xi_{ss'}$ = equivalent intervalley-scattering deformation potential,
- ν_s = number of equivalent (1,0,0) valleys,
- K_0, K_1 = modified Hankel functions.

To determine the unknown quantities k_{dc} , k_{ds} , T_c , T_s , and A_s/A_c , one utilizes^{10,3} the energy-balance equation

$$\langle d\epsilon/dt \rangle_{\text{coll},j} = \langle d\epsilon/dt \rangle_{\text{field},j} \quad (j=c, s); \quad (4)$$

the momentum-balance equation

$$\langle dp/dt \rangle_{\text{coll},j} = \langle dp/dt \rangle_{\text{field},j} \quad (j=c, s); \quad (5)$$

and, finally, the particle-balance equation

$$\langle dn/dt \rangle_{c \leftrightarrow s, c} = 0 \quad \text{or} \quad \langle dn/dt \rangle_{s \leftrightarrow c, s} = 0,$$

¹⁰ P. N. Butcher and W. Fawcett, Proc. Phys. Soc. (London) **86**, 1205 (1965).

from which A_s/A_c in Eq. (3) can be calculated using

$$\begin{aligned} \left\langle \frac{dn}{dt} \right\rangle_{c \rightarrow s, c} &\equiv \frac{(\Xi_{cs}/a_0)^2 \nu_s A_c}{2\rho\omega_{cs}} \frac{A_s}{q_c} \left\{ \frac{A_s}{A_c} \int_0^\infty [(N_{cs}+1)k_c(\epsilon+\Delta-\hbar\omega_{cs}) \right. \\ &\quad \times k_c^{2'}(\epsilon+\Delta-\hbar\omega_{cs}) + N_{cs}k_c(\epsilon+\Delta+\hbar\omega_{cs})k_c^{2'}(\epsilon+\Delta+\hbar\omega_{cs})] \exp\left(-\frac{\epsilon}{k_0T_s}\right) k_s(\epsilon)k_s^{2'}(\epsilon)d\epsilon \\ &\quad - \exp\left(-\frac{\Delta}{k_0T_c}\right) \int_0^\infty \left[N_{cs} \exp\left(\frac{\hbar\omega_{cs}}{k_0T_c}\right) k_c(\epsilon+\Delta-\hbar\omega_{cs})k_c^{2'}(\epsilon+\Delta-\hbar\omega_{cs}) + (N_{cs}+1) \exp\left(-\frac{\hbar\omega_{cs}}{k_0T_c}\right) \right. \\ &\quad \left. \left. + k_c(\epsilon+\Delta+\hbar\omega_{cs})k_c^{2'}(\epsilon+\Delta+\hbar\omega_{cs}) \right] \exp\left(-\frac{\epsilon}{k_0T_c}\right) k_s(\epsilon)k_s^{2'}(\epsilon)d\epsilon \right\}. \end{aligned}$$

A_c/q_c and A_s/q_s readily follow from the condition of normalization

$$q_c + \nu_s q_s = 1, \quad (6)$$

where

$$q_c = 4\pi A_c \int_0^\infty k_c^2(\epsilon)k_c'(\epsilon) \exp(-\epsilon/k_0T_c)d\epsilon$$

$$q_s = 4\pi A_s \int_0^\infty k_s^2(\epsilon)k_s'(\epsilon) \exp(-\epsilon/k_0T_s)d1\epsilon.$$

The numerical evaluation of the system of equations is most conveniently done by elimination of k_{dj} from Eqs. (4) and (5) for j equal to both c and s , and eventually of E from the remaining two equations. With T_c fixed, T_s is then computed from the final equation. From k_{dc} , the drift velocity v_{dc} is obtained according to

$$\begin{aligned} v_{cE} &= \frac{1}{\hbar} \frac{\partial \epsilon}{\partial k_{cE}} = \frac{2k_{cE}}{\hbar} \frac{d\epsilon}{dk_{cE}}, \\ v_{dc} &= \frac{\int f_c v_{cE} d^3k_c}{\int f_c d^3k_c} = \frac{8\pi k_{dc}}{3\hbar k_0 T_c} \frac{A_c}{q_c} \int_0^\infty \exp\left(-\frac{\epsilon}{k_0T_c}\right) \frac{k_c^3(\epsilon)}{k_c^{2'}(\epsilon)} d\epsilon. \end{aligned}$$

The subscript E denotes the vector component in the field direction.

TABLE I. Numerical values used for the parameters.

T_0	300°K
ρ	5.37 g/cm ³
s	5.22×10^8 cm/sec ^a
ϵ_0	12.53
ϵ_∞	10.82
Δ	0.36 eV
$m_c/m_0 (=a_1)$	0.067
a_2	0.040 eV ⁻¹ b
m_s/m_0	0.40
ν_s	3
ω_0	5.37×10^{13} rad/sec
$\omega_{cs} = \omega_{sc}$	4.54×10^{13} rad/sec
E_1	7 eV
Ξ_{cs}/a_0	1×10^8 eV/cm

^a Reference 4.
^b Reference 6.

¹¹ P. N. Butcher, Rept. Progr. Phys. 30, 97 (1967).

III. RESULTS AND DISCUSSION

The calculations were performed with the same numerical values of the parameters as used by Butcher,¹¹ compiled in Table I. The results are presented in Figs. 1–7. The full curves refer to the nonparabolic case with $\Xi_{cs}/a_0 = 5.3 \times 10^8$ eV/cm, and the broken curves to the parabolic case for the same intervalley deformation potential. To show the influence of Ξ_{cs}/a_0 , calculations were also carried out for another value of Ξ_{cs}/a_0 (1×10^8 eV/cm) in the nonparabolic case (dotted curves).

Figures 1 and 2 show the relative importance to the energy and momentum relaxation of the various scattering processes. In the *central valley* the energy transfer to the lattice is due to polar scattering below about 7 kV/cm and to nonequivalent intervalley scattering above [Fig. 1(a)]. The nonparabolicity enhances the effectiveness of polar scattering. When only polar scattering is considered, this effect of proper nonparabolicity [especially the nonparabolicity according to Eq. (1)] is well known to remove the dielectric breakdown present for parabolic band structure.⁸ Acoustical phonon scattering is always of minor importance, though it increases strongly with the mean electron energy (electron temperature; see Fig. 4) in the nonparabolic case. Accordingly, acoustical scattering is more intense for the lower Ξ_{cs} value, because of the larger electron temperature caused by diminished energy transfer to the satellite-valley electrons.

For the energy dissipation in the *satellite valleys* [Fig. 1(b)], polar scattering and equivalent and nonequivalent intervalley scattering all are important, being of the same order of magnitude. $\langle d\epsilon/dt \rangle_{s \rightarrow c, s}$ is positive, i.e., cs scattering, as well as the electric field, leads to heating of the (1,0,0) valley electrons. Therefore, at first glance, the influence of nonparabolicity is concealed because the effect on $\langle d\epsilon/dt \rangle_{\infty 11, s}$ is not illustrative of the individual contributions. Nevertheless, as a consequence of the relative relevance of cs scattering, the nonparabolicity indirectly affects the energy balance in the satellite valleys appreciably. An increase of the absolute value of cs scattering (by change of Ξ_{cs} or a_2) results in a reduction of the total energy dissipation to the lattice.

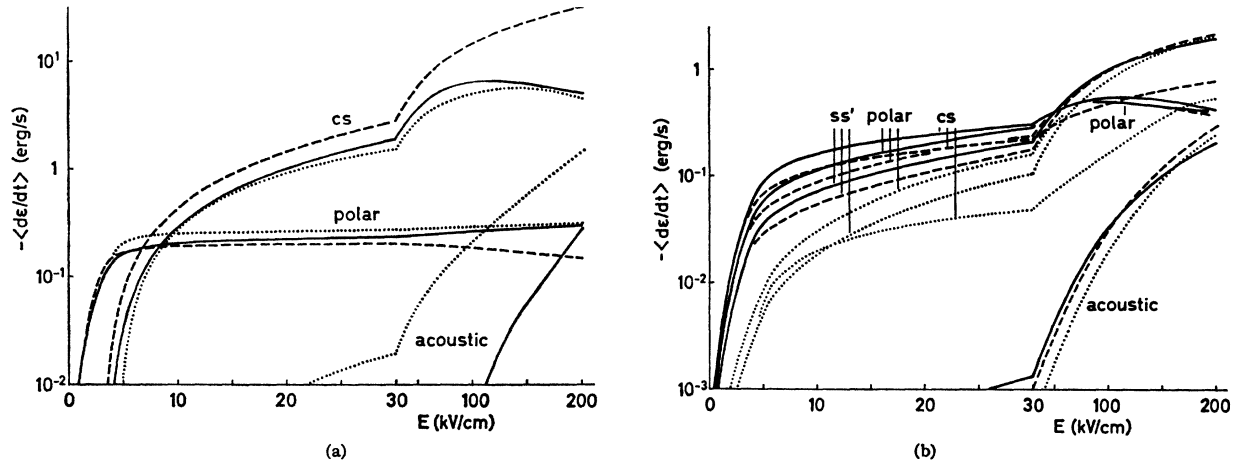


FIG. 1. Contribution of the various scattering mechanisms to the energy relaxation in the central (a) and the satellite valleys (b) as a function of the electric field E . ($d\epsilon/dt)_{s \leftrightarrow s, s}$ is positive. In all figures the full curves correspond to the nonparabolic case with $\Xi_{cs}/a_0 = 5.3 \times 10^8$ eV/cm, the broken curves to the parabolic case with the same Ξ_{cs}/a_0 , and the dotted curves to the nonparabolic case with $\Xi_{cs}/a_0 = 1 \times 10^8$ eV/cm.

This is apparent from Fig. 5 because the total energy dissipation is proportional to the mobility for fixed field [Eqs. (2) and (4)]. Energy relaxation via acoustical phonon scattering is also negligible in the satellite valleys.

Concerning the relative importance of the scattering processes to the *momentum* relaxation in the $(0,0,0)$ valley [Fig. 2(a)], qualitatively the same is true as for the energy relaxation. The only difference is that the acoustical-phonon scattering is more pronounced as compared with polar scattering, surpassing it at $E \sim 10^5$ V/cm. For the smaller value of Ξ_{cs}/a_0 (1×10^8 eV/cm), corresponding to a larger mean electron energy, the momentum relaxation due to acoustical-phonon scattering becomes so large as to exceed that due to cs scattering and, in contrast with the energy relaxation, the effect of cs scattering is sharply reduced.

In the *satellite valleys*, the momentum relaxation is essentially achieved by ss' and polar scattering [Fig. 2(b)]. cs scattering is of secondary importance. Therefore, nonparabolicity practically does not affect the momentum balance, which thus is a purely intravalley affair.

The results obtained on the relative significance for momentum relaxation of the various scattering mechanisms are in qualitative agreement with a discussion in terms of the scattering relaxation times.⁴

As compared with the parabolic case, nonparabolicity [Eq. (1)] is equivalent to an effective mass in the $(0,0,0)$ valley that increases with electron energy and thus concentrates the electrons at lower energies. This leads to a reduction of the electron transfer to the $(1,0,0)$ valleys at the same field value (Fig. 3). For the highest field strengths shown, there is even a depopulation of the

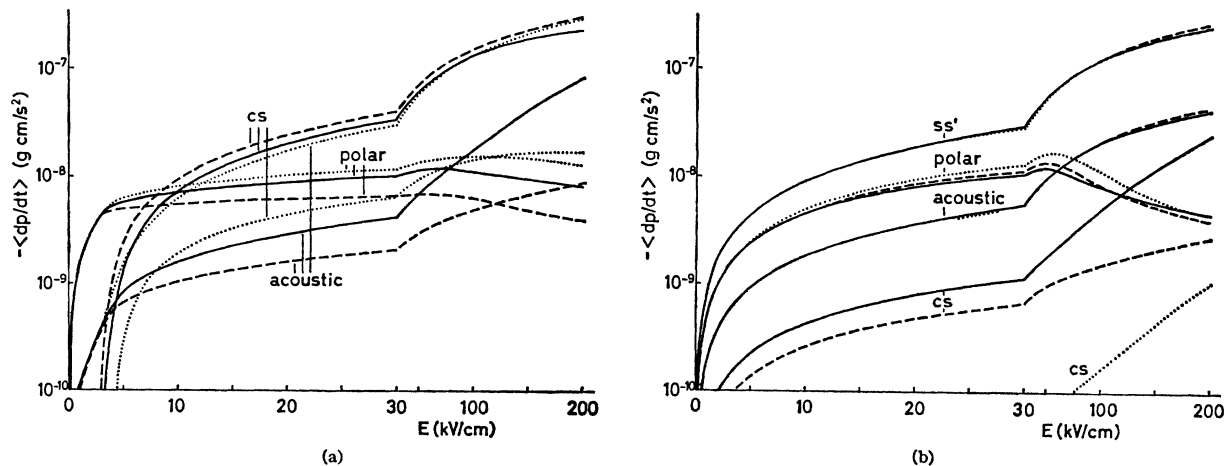


FIG. 2. Contribution of the various scattering mechanisms to the momentum relaxation in the central (a) and the satellite valleys (b) as a function of field E .

satellite valleys with rising field, which may be attributed to the increasing effective density of states in the central valley.

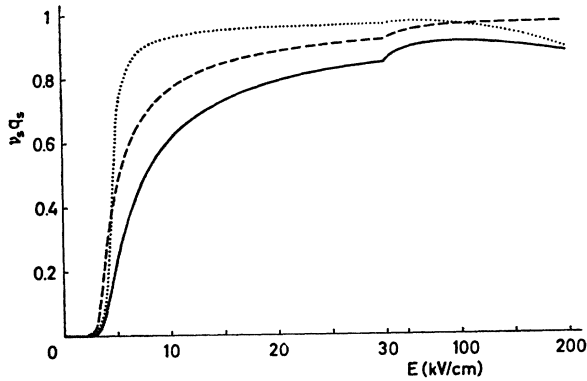


FIG. 3. Relative population of the satellite valleys $\nu_s q_s$, as a function of field E .

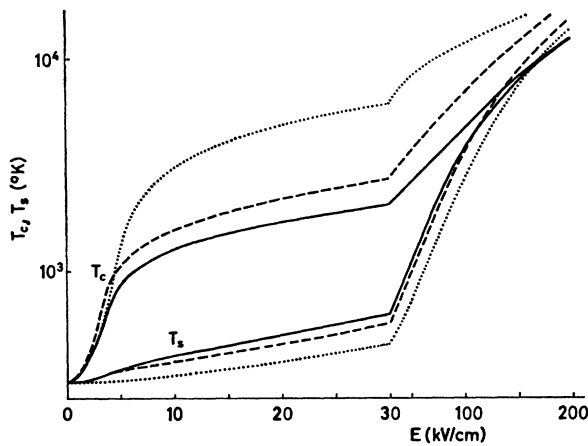


FIG. 4. Electron temperatures T_e, T_s as a function of field E .

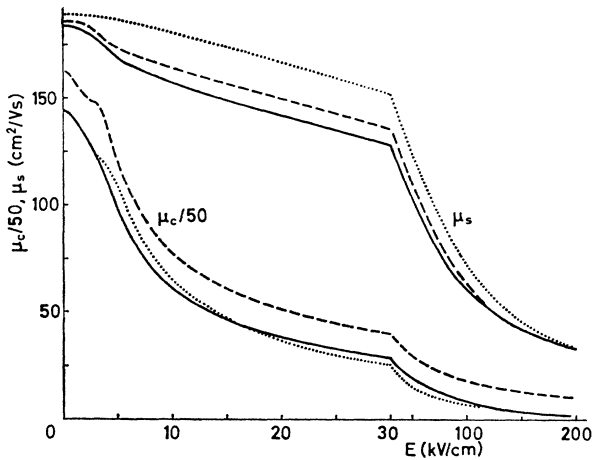


FIG. 5. Mobilities μ_c, μ_s as a function of field E .

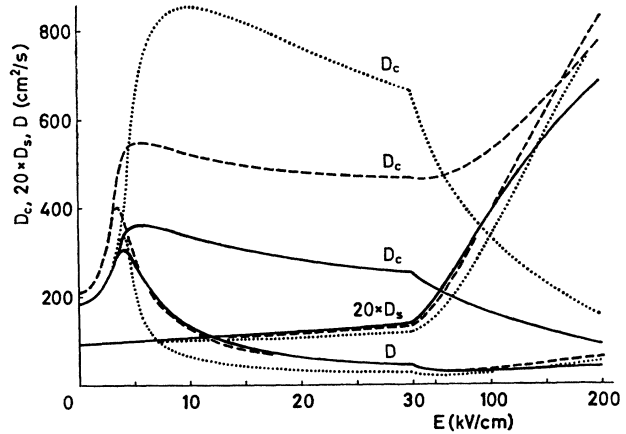


FIG. 6. Diffusion coefficients D_c, D_s, D as a function of field E

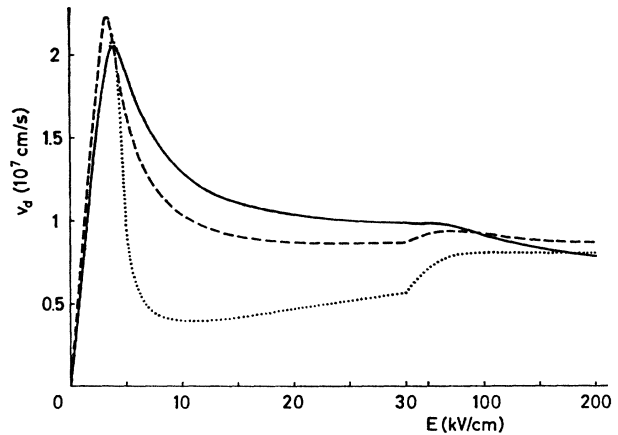


FIG. 7. Average drift velocity v_d as a function of field E .

Consistent with the concept of increasing effective mass is also the weaker increase of the central-valley electron temperature with field in the nonparabolic case (Fig. 4). In contrast, the temperature of the satellite-valley electrons rises more rapidly, which is ascribed to stronger heating by intervalley transfer [Fig. 1(b)]. Because this effect decreases with the magnitude of the coupling constant Ξ_{cs} , for $\Xi_{cs}/a_0 = 1 \times 10^8$ eV/cm the increase of T_s is less marked. With reduced coupling to the satellite valleys, the energy transfer to the lattice of the (0,0,0) valley electrons via cs scattering also drops [Fig. 1(a)], thus accounting for the stronger increase of T_e with field than that shown in the full-line curve ($\Xi_{cs}/a_0 = 5.3 \times 10^8$ eV/cm).

Nonparabolicity also lowers the mobility in the central valley, even for fields $E \rightarrow 0$ (Fig. 5), which is to be expected from the viewpoint of increased effective mass of the high-energy electrons. This result has also been found in the quasi-elastic approach.^{1,2} Even the mobility in the (1,0,0) valleys is somewhat affected by nonparabolicity of the (0,0,0) valley and the magnitude of the

scattering constant Ξ_{cs} . This is attributed to the noticeable influence of these quantities on the *energy* relaxation in the satellite minima, and cannot be understood from their negligible contribution to the *momentum* relaxation.

The field dependence of the mobilities and electron temperatures may be used to calculate the diffusion coefficients as a function of field with the aid of the Einstein relation

$$D_j = k_0 T_j \mu_j / e, \quad j = c \text{ and } s$$

$$D = q_c D_c + \nu_s q_s D_s,$$

where D is the average diffusion coefficient (see Fig. 6). The dependence of $D_s(E)$ on nonparabolicity and Ξ_{cs} is relatively small—the more so inasmuch as the effects of μ_s and T_s (Figs. 4 and 5) partially compensate each other. The influence on D_c is considerable. The initial increase with field is due to the increasing electron temperature; the decrease at large field values in the nonparabolic case, to the strongly reduced mobility. The behavior of $D_c(E)$ at fields $\gtrsim 30$ kV/cm expresses the effect of nonparabolicity most clearly. As compared with the approximation of Conwell and Vassell,¹ the shifting of the $D_c(E)$ curves due to nonparabolicity and the effect of Ξ_{cs} is in the same direction, but the numerical agreement is very poor. However, the agreement is rather good concerning the average diffusion coefficient $D(E)$.

From the curves for $\nu_s q_s$ and for μ_c and μ_s , the average drift velocity $v_d = (q_c \mu_c + \nu_s q_s \mu_s) E$ follows, which is of basic interest in the Gunn effect (Fig. 7). Comparison with the experimental results due to Ruch and Kino¹²

¹² J. G. Ruch and G. S. Kino, Appl. Phys. Letters **10**, 40 (1967).

has been made earlier.¹³ The nonparabolic curve ($\Xi_{cs}/a_0 = 5.3 \times 10^8$ eV/cm) shows a very flat minimum at $E = 39$ kV/cm and continues to drop beyond that field. As distinguished from the parabolic curve,³ the threshold field is at 4.0 kV/cm (parabolic: 3.3 kV/cm). The maximum drift velocity, the maximum negative differential mobility, and the zero-field mobility are lowered as compared with the parabolic curve. Qualitatively, these differences may be considered to be not severe. A larger variation, however, is caused by the smaller value of 1×10^8 eV/cm for Ξ_{cs}/a_0 . A curve results (dotted) that exhibits a considerably larger drift-velocity peak-to-valley ratio and maximum negative differential mobility, as is consistent with experiments. Moreover, the characteristic turns markedly upward past the valley field (whose value as given by the theory is probably too low—another deficiency), thus predicting flat-topped Gunn domains¹⁴ with a saturation field of ~ 40 kV/cm, the existence of which has not been verified so far.¹⁵ Experiments rather give domain maximum fields in excess of 10^5 V/cm.^{15,16} For this reason, a nonequivalent-intervalley-scattering deformation-potential constant of $\Xi_{cs}/a_0 \sim 1 \times 10^8$ eV/cm seems to be too low for GaAs. Such a value has been suggested by Conwell and Vassell¹⁷ in order to interpret the low-field ionization postulated by Copeland.¹⁸

¹³ W. Heinle, Phys. Letters **27A**, 629 (1968).

¹⁴ P. N. Butcher, W. Fawcett, and C. Hilsum, Brit. J. Appl. Phys. **17**, 841 (1966).

¹⁵ J. B. Gunn, IEEE Trans. Electr. Dev. **ED-14**, 720 (1967).

¹⁶ I. Kuru, P. N. Robson, and G. S. Kino, IEEE Trans. Electr. Dev. **ED-15**, 21 (1968).

¹⁷ E. M. Conwell and M. O. Vassell, J. Phys. Soc. Japan, Suppl. **21**, 527 (1966).

¹⁸ J. A. Copeland, Appl. Phys. Letters **9**, 140 (1966).